ORIGINAL RESEARCH

Understanding the translocation mechanism of PLGA nanoparticles across round window membrane into the inner ear: a guideline for inner ear drug delivery based on nanomedicine

Liping Zhang[1–3]
Yuan Xu[1]
Wenjuan Cao[1]
Shibao Xie[1–3]
Lu Wen[1]
Gang Chen[1–3]

[1]School of Pharmacy, [2]Guangdong Provincial Key Laboratory of Advanced Drug Delivery, [3]Guangdong Provincial Engineering Center of Topical Precise Drug Delivery System, Guangdong Pharmaceutical University, Guangzhou, China

Background: The round window membrane (RWM) functions as the primary biological barrier for therapeutic agents in the inner ear via local application. Previous studies on inner ear nano-drug delivery systems mostly focused on their pharmacokinetics and distribution in the inner ear, but seldom on the interaction with the RWM. Clarifying the transport mechanism of nanoparticulate carriers across RWM will shed more light on the optimum design of nano-drug delivery systems intended for meeting demands for their clinical application.

Methods: The poly (lactic-co-glycolic acid) nanoparticles (PLGA NPs) encapsulating coumarin-6 were prepared by emulsifying solvent evaporation method. We utilized confocal laser scanning microscope (CLSM) in combination with transmission electron microscope to investigate the transport pathway of PLGA NPs in the RWM. Simultaneously, the concentration and time dependence of NPs across the RWM were also determined. The endocytic mechanism of NPs through this membrane interface was classically analyzed by means of various endocytic inhibitors. The intracellular location of NPs into lysosomes was evaluated using CLSM scanning microscope colocalization analysis. The Golgi-related inhibitors were employed to probe into the function of Golgi and endoplasmic reticulum (ER) in the discharge of NPs out of cells.

Results: PLGA NPs were herein transported through the RWM of a sandwich-like structure into the perilymph via the transcellular pathway. NPs were internalized predominantly via macropinocytosis and caveolin-mediated endocytic pathways. After being internalized, the endocytosed cargos were entrapped within the lysosomal compartments and/or the endoplasmic reticulum/Golgi apparatus which mediated the exocytotic release of NPs.

Conclusion: For the first time, we showed the translocation itinerary of NPs in RWM, providing a guideline for the rational fabrication of inner ear nanoparticulate carriers with better therapeutic effects.

Keywords: poly (lactic-co-glycolic acid) nanoparticles, round window membrane, endocytotic mechanism, exocytotic mechanism, inner ear

Correspondence: Lu Wen; Gang Chen
School of Pharmacy, Guangdong Pharmaceutical University, 280 Waihuan East Road, Guangzhou Higher Education Mega Center, Guangzhou 510006, China
Tel +86 20 3935 2141; +86 20 3935 2117
Fax +86 20 3935 2129
Email gywenl@163.com;
cg753@126.com

Introduction

The inner ear possesses two key components, the cochlea and the vestibule, as a challenging target for drug delivery to combat hearing-related diseases and balance dysfunction, respectively. Topical administration of medicines via the round window membrane (RWM) was favored by otologists due to efficacy, noninvasive delivery, bypassing of the blood–perilymph barrier, and reduced toxicity to nontargeted tissues compared to systemic administration.[1] RWM, a primary interface to the inner ear, is a sandwich-like

structure that comprises three layers: an outer epithelium layer orientating the middle ear, a layer of connective tissue, and an inner epithelium layer facing the scala tympani.[2] RWM has two functions: 1) as a selective filter to control the absorption and secretion of substances from and to the scala tympani[3] and 2) as a "defense system" to circumvent the entry of toxicants. Drugs with low molecular weight and high lipid solubility can traverse RWM readily, while the others cannot.[4] Thus, it is pivotal to conquer the RWM barrier and to enhance the transport efficiency of low-permeability drugs.

In recent years, nanotechnology has become one of the primary strategies to address the epithelium barrier.[5] Poly (lactic-co-glycolic acid) nanoparticles (PLGA NPs) for delivering drugs to the inner ear are becoming increasingly popular due to their biocompatibility, biodegradability, and ability to sustain therapeutic drug concentration for an extended period. Compared to free drugs, encapsulating them into PLGA NPs can facilitate entry into the perilymph, thus promoting drug local bioavailability, which was demonstrated in our previous study.[6] Researchers have endeavored to treat inner ear diseases using PLGA NPs in the past few decades, but the mechanisms behind their transport across RWM remain elusive.[7–9] The endocytosis mechanism of NPs has been well investigated in various biological barriers such as the respiratory airway, gut, renal proximal tubule, and corneal epithelium.[10–14] Thus, a better understanding of the important biological processes that dictate the fate of PLGA NPs across RWM raises hope in terms of more effective individualized platforms.

This study aimed to explore and investigate the interaction of PLGA NPs with RWM barrier, including the permeability, endocytosis pathway, and intracellular itinerary, as well as the exocytosis mechanism underlying RWM absorption. First of all, coumarin-6 emitting green fluorescence was encapsulated in PLGA NPs and distributed extensively in the RWM by confocal laser scanning microscope (CLSM) with z-axis scanning model, in combination with particles in the perilymph under transmission electron microscope (TEM) observation after intratympanic injection of the NPs, which fully verified that the NPs could transport through the RWM into the inner ear. Meanwhile, the outer epithelium layer, connective tissue layer, and inner epithelium layer of the confocal sequential z-axis images of RWM were distinguished by scanning electron microscopy (SEM). The time and concentration dependences of PLGA NP transport across the semipermeable membrane were evaluated by quantifying the coumarin-6 fluorescence intensity in RWM using CLSM. Secondly, when NPs worked through the membrane barrier, the outer epithelium layer acted as the main epithelium barrier.[3] Substances may cross epithelium barriers along two ways: transcellular or paracellular pathway.[15] The TEM images of RWM determined which one was the dominant role mediating the entry of PLGA NPs into RWM. NPs are endocytosed following three different mechanisms, that is, macropinocytosis, caveolin-mediated endocytosis, and clathrin-mediated endocytosis.[16] Endocytosis inhibitors ascribed to specific endocytic pathways were used to investigate the endocytosis pathway of PLGA NPs. Finally, after being internalized, the endocytosed cargos were transferred to various cellular organelles, including lysosomes, the endoplasmic reticulum (ER), and Golgi apparatus. The entrapment of NPs into lysosomes was evaluated using CLSM colocalization analysis software. Golgi apparatus-related inhibitors revealed that the Golgi apparatus and ER mediated the discharge of NPs outside cells. The large extracellular space facilitated the passage of PLGA NPs across the connective tissue layer and inner epithelium layer of RWM. Thus, only the outer epithelium layer was taken into consideration in investigating NP transport across the RWM for simplification.

Materials and methods
Chemicals and animals
Coumarin-6 was purchased from Sigma-Aldrich Co (St Louis, MO, USA). PLGA (lactic acid/glycolic acid =75:25, molecular weight [MW] 10 kDa) was supplied by Shandong Medical Institute (Shandong, China). Chlorpromazine hydrochloride, monensin sodium salt (MON), and colchicine were purchased from Aladdin Reagent (Shanghai, China). Methyl-β-cyclodextrin (MβCD) was purchased from Macklin Reagent (Shanghai, China). Brefeldin A (BFA) was purchased from MedChemExpress (Princeton, NJ, USA). 4′,6-Diamidino-2-phenylindole (DAPI) and LysoTracker Red were purchased from Beyotime Institute of Biotechnology (Shanghai, China). Albino guinea pigs (300–350 g) were obtained from the Laboratory Animal Center of Southern Medical University (Guangzhou, China). All animal studies were performed with humane care in accordance with the protocols approved by the National Institutes of Health Guide for the Care and Use of Laboratory Animals. The Animal Ethical Committee on the Care and Use of Laboratory Animals (Guangdong Pharmaceutical University, Guangzhou, China) approved this study.

NPs preparation and characterization
NPs containing coumarin-6 were prepared by emulsion solvent evaporation method according to our previously published experimental procedure.[6] In brief, 30 mg of PLGA and 60 µg of coumarin-6 in 1 mL of dichloromethane/ethyl acetate (7:3) were added into 5 mL of 3% (w/v) polyvinyl alcohol (PVA)

aqueous solution on ice using a probe sonicator set at 190 W in pulse mode to create an oil-in-water emulsion (Scientz Biotechnology Co, Ltd, China). Then, this emulsion was diluted with a 0.5% (w/v) PVA aqueous solution, and immediately stirred with a magnetic stirrer to allow for organic solvent evaporation. The NPs were then collected by centrifugation followed by freeze drying and stored at 25°C. NP size was analyzed using Zetasizer Nano-S90 (Malvern Instruments, Malvern, UK). Delsa TM Nano C was used for the zeta potential analyses of particles (Beckman Coulter Instruments, Brea, CA, USA). The particles size and zeta potential of PLGA NPs were 160.3 nm (polydispersity index =0.189) and −12.12 mv.

CLSM imaging of RWM

To monitor whether NPs could be transported through the RWM, guinea pigs were executed with 20% urethane and bullae were harvested after intratympanic injection of 0.1 mL of 90 mg/mL PLGA NPs for 30 minutes. Then, the bullae were fixed overnight at 4°C in 4% formaldehyde in phosphate-buffered saline (PBS). After another 5 minutes of washing in PBS, RWM samples were microdissected with tweezers under a stereomicroscope, and incubated with DAPI for 20 minutes to visualize the cell nucleus. After washing with PBS, RWMs were placed on glass slides in glycerin and coverslipped. Finally, the coverslips were sealed with nail polish to protect the specimens from desiccation and examined by CLSM (LSM 710 Meta; Carl Zeiss Meditech AG, Jena, Germany) in the x-y-z scanning mode using a 63× oil objective. The excitation wavelengths of DAPI and coumarin-6 were set at 405 and 458 nm, respectively.

The concentration and time dependences of NPs across RWM were also evaluated by CLSM. Afterward, 0.1 mL of 10, 30, and 90 mg/mL PLGA NPs were intratympanically injected, respectively (n=3), for 30 minutes to evaluate the concentration dependence. For the time dependence experiment, 0.1 mL of 90 mg/mL PLGA NPs was intratympanically injected for 10, 30, and 60 minutes, respectively (n=3). Then, the guinea pigs were executed and RWM surface preparation was conducted as mentioned above. RWM samples were observed with CLSM in the z-stack scanning mode with a step size of 1 μm. A 63× oil objective was used. The excitation wavelengths of DAPI and coumarin-6 were set at 405 and 458 nm, respectively.

The intracellular location of NPs in lysosomes was also investigated by CLSM. The guinea pigs were executed following intratympanic injection of 0.1 mL of 90 mg/mL PLGA NPs for 30 minutes. Then, the bullae were harvested and fixed overnight. RWM samples were microdissected and incubated with DAPI for 20 minutes to visualize the cell nucleus. For counterstaining, RWM samples were stained with LysoTracker Red to selectively label lysosomes, and incubated for an additional 2 hours at 37°C. Then, RWM surface preparation was conducted as mentioned above and observed with CLSM in the z-stack scanning mode with a step size of 1 μm. A 63× oil objective was used. The excitation wavelengths of DAPI, coumarin-6, and LysoTracker Red were set at 405, 458, and 543 nm, respectively. The colocalization of lysosomes and NPs was analyzed using the built-in Carl Zeiss colocalization analysis software.

TEM

NP movement across epithelium barriers occurs through the transcellular pathway and/or the paracellular pathway. To determine which pathway dominantly mediated the transport of PLGA NPs in RWM, RWM samples were prepared for TEM. Specifically, guinea pigs were assigned to two groups: 1) untreated group; 2) intratympanic injection of PLGA NPs for 30 minutes group (0.1 mL, 90 mg/mL). Then, the guinea pigs were executed with 20% urethane. After the animals were decapitated, the temporal bones were trimmed of excess bone and tissue. After glutaraldehyde fixing of all bullae for 12 hours, the samples were decalcified with ethylene diamine tetraacetic acid (EDTA) solution for 7 days and rinsed several times by buffer. RWM surrounded by a ring of hard bone was harvested, postfixed in 1% osmium tetroxide for 2 hours at 4°C, dehydrated, and embedded in Spurr's resin. Sections were cut into thicknesses of 50–70 nm with glass knives using an ultramicrotome (Leica UC7; Leica Microsystems, Wetzlar, Germany), stained with uranyl acetate-lead citrate, and examined with TEM (Hitachi H-7500; Hitachi Ltd, Tokyo, Japan).

To investigate whether NPs traversed the RWM to the perilymph, guinea pigs were divided into two tympanic treatment groups: PLGA NPs (group I, 90 mg/mL, 0.1 mL) treatment for 30 minutes and PBS (group II, 0.1 mL) treatment for 30 minutes. PLGA NPs suspension was used as the positive control. The perilymph was sampled under general anesthesia, followed by a lethal intraperitoneal injection of urethane. Glass capillaries were inserted to the RWM after proper exposure of the cochlea, and perilymph samples (5 μL) were withdrawn. Then, the samples were mounted on the copper grids. After absorption for 10 minutes, the copper grids were stained by 0.2% phosphotungstic acid and samples were observed using TEM (Hitachi H-7650).

Inflammatory reactions upon multiple pharmacological regulators

Sixty minutes after intratympanic administration of inhibitor solutions, guinea pigs were anesthetized with 20% urethane.

Bullae were removed, fixed overnight at 4°C in 4% formaldehyde in PBS, and decalcified in 0.1 mol/L EDTA for 7 days. The cochlea was trimmed and embedded for modiolus section. Then, 5-µm thick sections were cut, stained with hematoxylin and eosin, and examined under a fluorescence microscope (Zeiss Axio Scope A1; Carl Zeiss Meditech AG).

High-performance liquid chromatography (HPLC)

When NPs adhere on the RWM surface, endocytosis by cells in the outer epithelium is a prerequisite for the entry of NPs into RWM. Various endocytosis inhibitors were utilized to elucidate the endocytosis mechanisms of NPs. Colchicine (40 µg/mL) was utilized as the macropinocytosis-inhibitory agent;[17] MβCD (10 mmol/L) as the inhibitor of caveolae-mediated endocytosis;[11] and chlorpromazine hydrochloride (100 µg/mL) as the clathrin inhibitor.[18] BFA (50 µg/mL) and MON (32.5 µg/mL), as Golgi apparatus-related inhibitors, were employed to evaluate the impact of Golgi apparatus on the exocytosis of NPs.[11] Guinea pigs were pretreated for 30 minutes by intratympanic injection of 0.1 mL of various agents. After the aspiration of inhibitors solutions, guinea pigs were further treated for 30 minutes by intratympanic injection of 0.1 mL of 30 mg/mL NPs containing inhibitor solutions with the same concentrations. Then, 5 µL of perilymph samples were collected as described. For perilymph samples preparation, after adding 50 µL of methanol to 5 µL of each perilymph, the mixture was centrifuged (10 minutes at 9,000 g) and 20 µL of clear supernatant were injected into the HPLC system (Shimadzu Corporation, Kyoto, Japan) equipped with a Dikma Diamonsil C_{18} column (150×4.6 mm, 5 µm; Dikma Technologies Inc, Lake Forest, CA, USA), a fluorescence detector (RF-10AXL), and a pump (LC-10ATvp). The excitation and emission wavelengths were set at 466 and 504 nm, respectively. At the column temperature of 35°C, 20 µL of samples were eluted by a mobile phase consisting of acetonitrile and water (80:20, v/v) at a flow rate of 1 mL/min. The peak area of coumarin-6 was recorded at the retention time of 7 minutes.

To assess whether coumarin-6 could be utilized as an effective marker of NPs, the in vitro leakage of coumarin-6 from PLGA NPs was tested using the dialysis bag method. Briefly, 0.09 g PLGA NPs were suspended in 1 mL of PBS at pH 7.2 and pH 5.5, respectively. Then, the NPs dispersion was added in a dialysis bag (MW cutoff 30 kDa) and dialyzed against 20 mL of release medium similarly as the solution within the dialysis bag. At 100 rpm and 37°C, 0.5 mL of release medium was removed at 0.5, 1, 2, 4, 6, 8, 12, and 24 hours, and detected by HPLC as described earlier.

SEM

To observe the morphology of RWM, RWM samples of untreated guinea pigs were prepared for SEM. Normal guinea pigs were executed with 20% urethane, from which RWM samples were harvested, fixed with glutaraldehyde, and rinsed several times with buffer. RWM samples surrounded by a ring of hard bone were harvested and postfixed in 1% osmium tetroxide. Following a PBS rinse, the samples were dehydrated, critical-point-dried with CO_2 (Hitachi HCP-5), coated with gold (Hitachi E-1020), and examined with SEM (Hitachi S-3000N).

Statistics

All statistical analyses were performed using IBM SPSS 19.0 software (IBM Corporation, Armonk, NY, USA) to determine variance with Tukey multiple comparison tests. All data were expressed as mean value ± SD. A p-value <0.05 was considered to be statistically significant.

Results
Identification of three layers of RWM by CLSM

To understand the migration of PLGA NPs from the middle ear side to the scala tympani side of the membrane barrier, the z-stack series images of RWM were obtained by CLSM in the z-stack scanning mode with a step size of 1 µm. The outer epithelium layer, connective tissue layer, and inner epithelium layer of RWM z-stack series images were differentiated by SEM. The outer epithelium cells were arranged densely and there were cell junctions, corresponding to the bright field confocal images at a depth of 0–4 µm; in the connective tissue layer, collagenous fibers were in an interlaced array, similar to the bright field confocal images at a depth of 5–12 µm; inner epithelium cells were arrayed loosely (Figure 1). Based on the SEM images of RWM, three layers of RWM confocal z-stack series images were easily distinguished. The shapes of DAPI-stained cell nuclei in the outer epithelium layer, connective tissue layer, and inner epithelium layer were oval, long striped, and oval, respectively, as additional determination criteria (Figure 2A). Thus, the outer epithelium layer, connective tissue layer, and inner epithelium layer were located at 0–4, 5–12, and 12–23 µm, respectively.

NP transport across RWM into the inner ear

RWM serves as the main biological barrier between the middle ear and inner ear. To study the distribution of PLGA
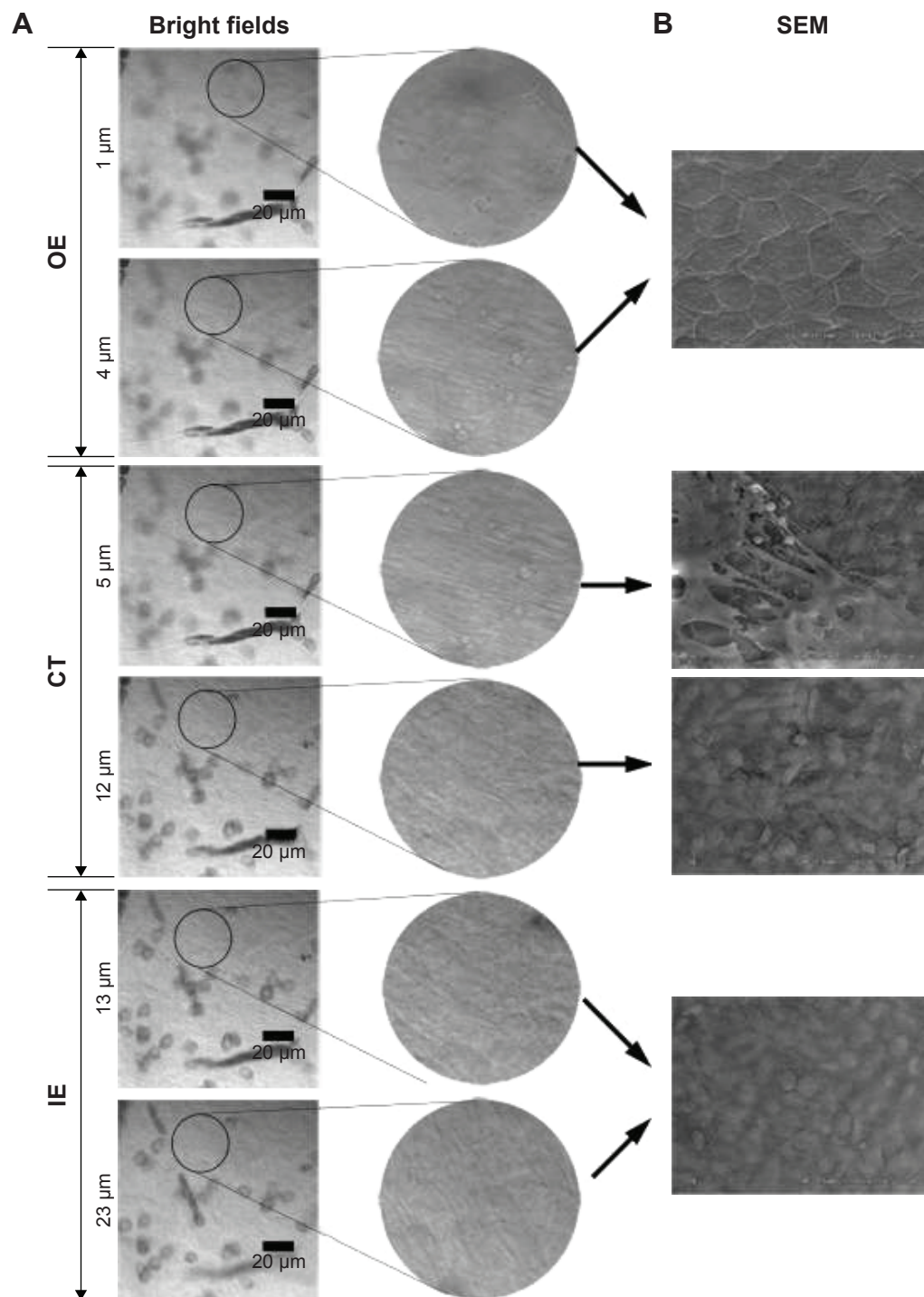
A **Bright fields**

B **SEM**

Figure 1 Bright field confocal images of RWM in the x-y-z scanning mode (**A**). SEM images of RWM (**B**).
Abbreviations: RWM, round window membrane; SEM, scanning electron microscope; OE, outer epithelium layer; CT, connective tissue; IE, inner epithelium layer.

NPs in this membrane interface, RWM samples were scanned layer-by-layer using CLSM with the z-stack scanning model after intratympanic injection of PLGA NPs. PLGA NPs indicated by the green fluorescence of coumarin-6 in looping structures throughout the cytoplasm migrated from the middle ear side to the scala tympani side of

RWM (Figure 2A). As evidenced by the three-dimensional reconstruction image of RWM obtained from successive z-stacks, PLGA NPs represented by green spots were distributed overwhelmingly throughout the RWM (Figure 2B). Figure 2C shows the fluorescence intensities of PLGA NPs in three layers.

Figure 2 CLSM of RWM after intratympanic injection of PLGA NPs. (**A**) CLSM series images of RWM by the z-axis scanning model at 1-μm vertical intervals from middle ear side to scala tympanic side. DAPI-stained cell nuclei are seen in blue and PLGA NPs are seen in green. (**B**) Three-dimensional reconstruction image of RWM obtained from successive z-stacks. The green dots represent PLGA NPs. (**C**) Fluorescence intensity of the planar cross-sections of RWM from middle ear side to inner ear side of RWM with a step size of 1 μm.
Abbreviations: CLSM, confocal laser scanning microscope; RWM, round window membrane; PLGA NPs, poly (lactic-co-glycolic acid) nanoparticles; DAPI, 4′,6-diamidino-2-phenylindole; OE, outer epithelium layer; CT, connective tissue; IE, inner epithelium layer.

The distribution of PLGA NPs in the inner ear space is the precondition for the application of NPs in inner ear diseases therapy. To elucidate the passage of PLGA NPs across RWM into the inner ear, perilymph was detected by TEM. Compared to the TEM image of PLGA NPs (Figure 3A), there were homologous, sparse, intact particles in the perilymph after intratympanic injection of PLGA NPs (Figure 3B), further confirming that they passed through RWM into the inner ear. There were no particles in the perilymph sample of the blank control group (Figure 3C).
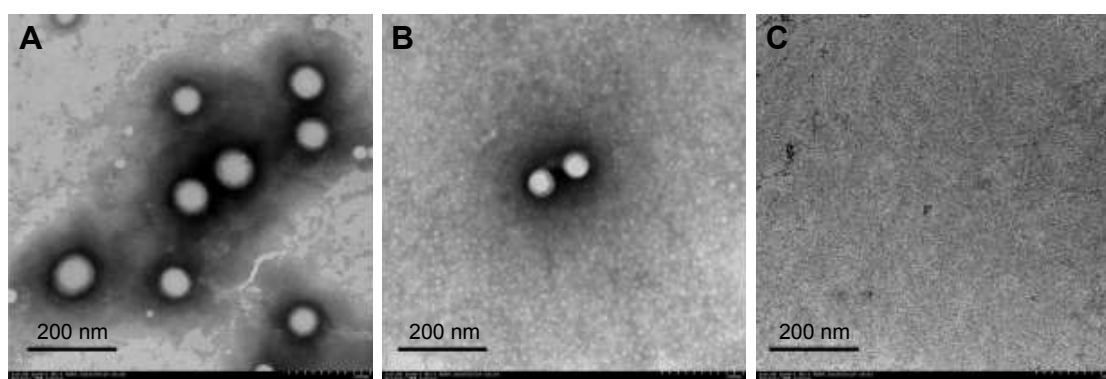

Figure 3 TEM image of PLGA NPs (**A**). TEM images of perilymph in the experimental group after intratympanic injection of PLGA NPs for 30 minutes (**B**) and blank group (**C**).
Abbreviations: TEM, transmission electron microscope; PLGA NPs, poly (lactic-co-glycolic acid) nanoparticles.
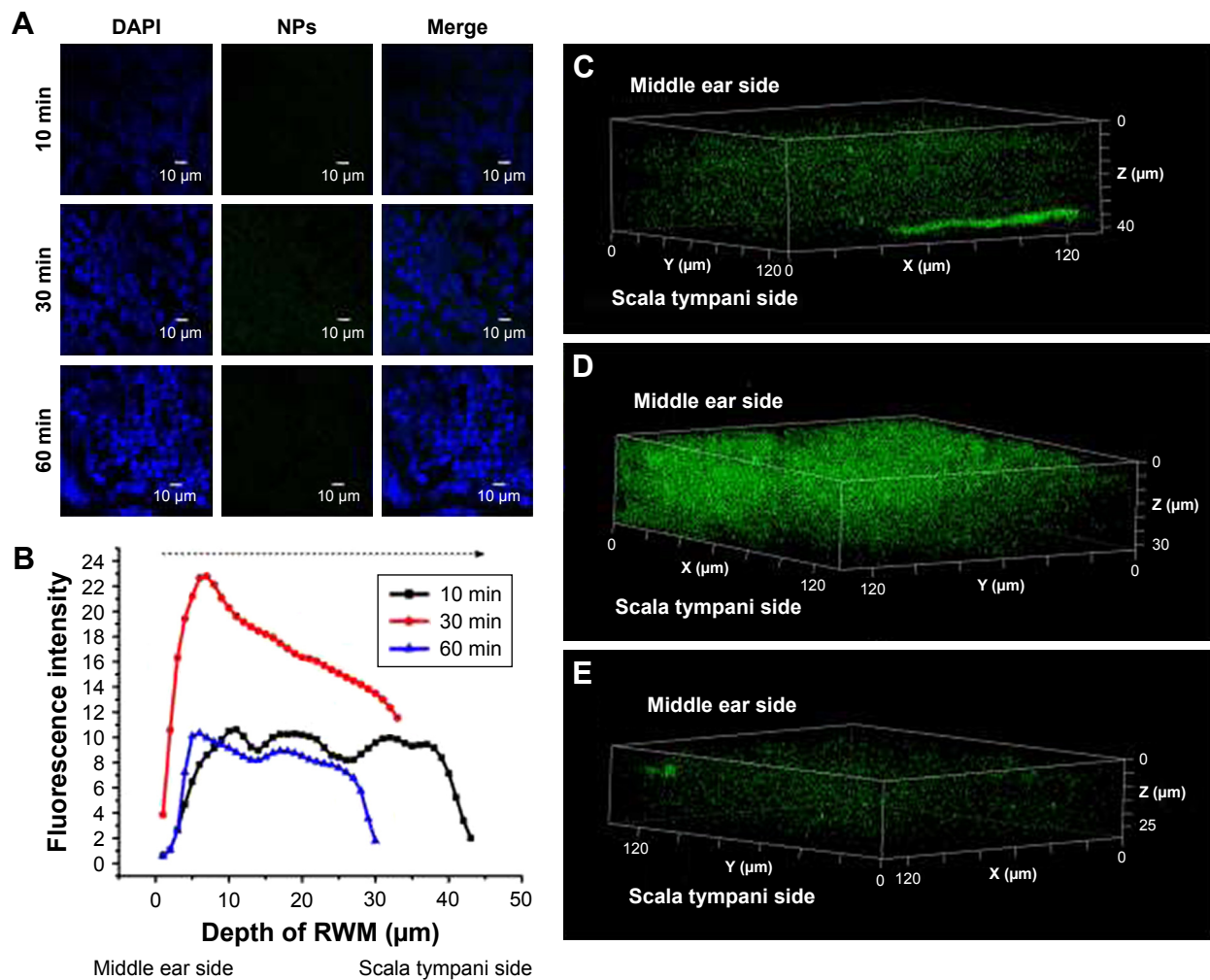
Figure 4 CLSM of RWM as a function of administration time. (**A**) CLSM micrographs of outer epithelium cells of RWM after intratympanic injection of 0.1 mL of 90 mg/mL PLGA NPs for 10, 30, and 60 minutes. DAPI-stained cell nuclei are blue and PLGA NPs are green. (**B**) Coumarin-6 fluorescence intensity of RWM at different distances along the z-axis from middle ear side to inner ear side. Three-dimensional reconstruction images of RWM obtained from successive z-stacks after intratympanic injection of NPs for 10 minutes (**C**), 30 minutes (**D**), and 60 minutes (**E**).
Abbreviations: CLSM, confocal laser scanning microscope; RWM, round window membrane; DAPI, 4′,6-diamidino-2-phenylindole; PLGA NPs, poly (lactic-co-glycolic acid) nanoparticles.

The coumarin-6 fluorescence intensity in RWM increased gradually with time from 10 to 30 minutes, and then dropped at 60 minutes (Figure 4). Raising the concentration of PLGA NPs enhanced the coumarin-6 fluorescence intensity in RWM, revealing that PLGA NPs entered RWM in a concentration-dependent manner and most NPs were found in the RWM at 90 mg·mL^{-1} (Figure 5).

Primary route mediating PLGA NP transport across RWM

Figure 6A and B shows the subcellular characteristics of the outer and inner epithelium layers of RWM in the control group. In contrast, the experimental group underwent a series of active uptake events including both endocytic and exocytic processes (Figure 6C–F). Typical and successive

endocytic behaviors, such as endocytic pits and subsequent endocytic vesicles, were observed (Figure 6C), indicating the vesicular transport pathway of NPs across RWM. Tight junctions in close proximity to the membrane invagination were not disrupted, restricting the paracellular pathway of NPs across RWM, as illustrated in Figure 6D.

Endocytosis mechanism of PLGA NP transport across RWM

The endocytosis mechanism of PLGA NPs across RWM was clarified with different endocytosis inhibitors. The safety of all the pharmacological inhibitors was evaluated by paraffin sections of RWM (Figure 7). Colchicine and MβCD decreased the NP transport amount in the perilymph, suggesting that the internalization of NPs was regulated by the macropinocytosis
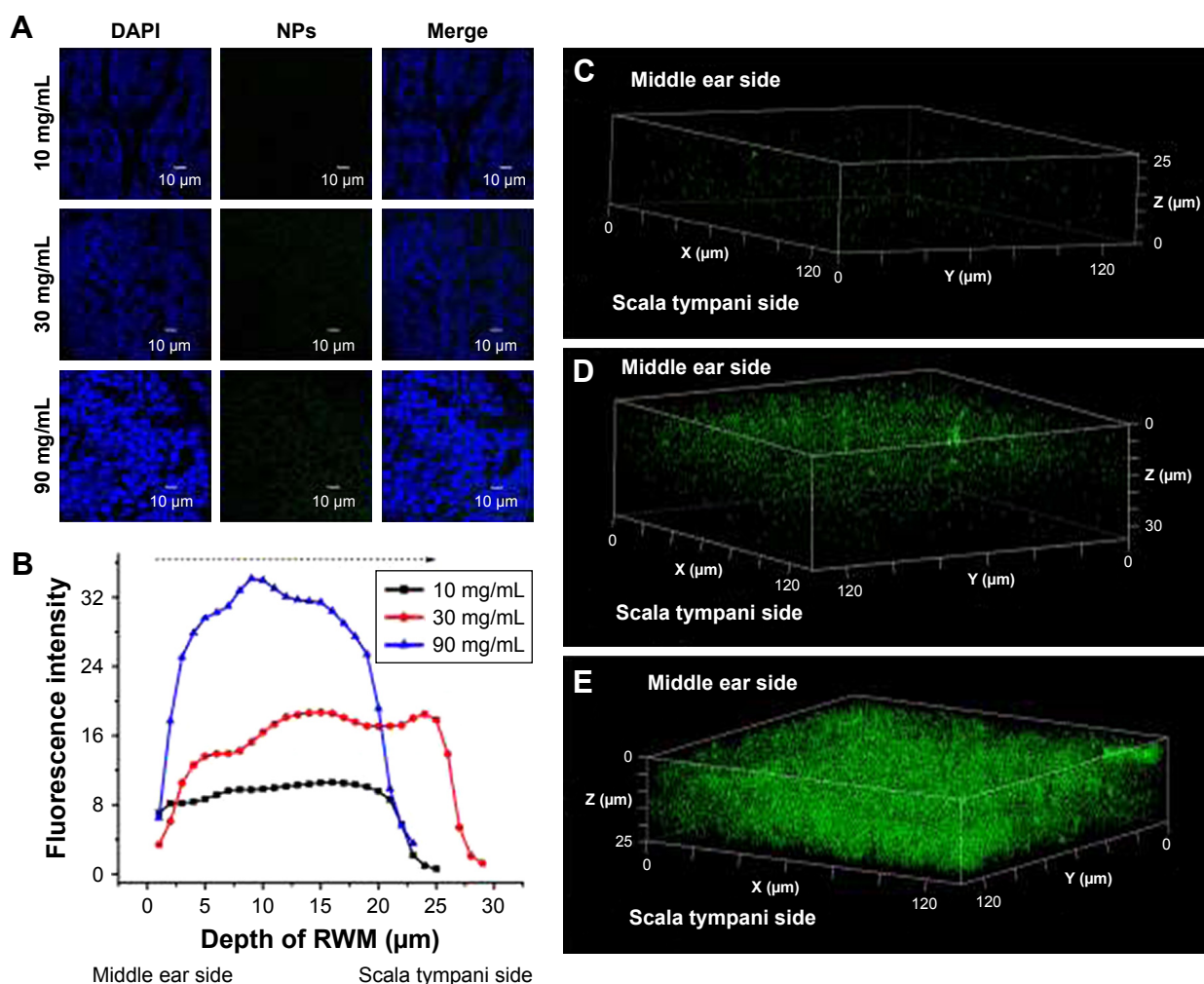
Figure 5 CLSM of RWM as a function of concentration. (**A**) CLSM micrographs of outer epithelium cells of RWM after intratympanic injection of 0.1 mL of 10, 30, and 90 mg/mL PLGA NPs for 30 minutes. (**B**) Coumarin-6 fluorescence intensities in the cross-section of RWM along the z-axis with 1-μm vertical intervals after intratympanic injection of PLGA NPs at different concentrations for 30 minutes. Three-dimensional reconstruction images of RWM obtained from successive z-stacks after intratympanic injection of 10 mg/mL (**C**), 30 mg/mL (**D**), and 90 mg/mL (**E**) PLGA NPs for 30 minutes.

Abbreviations: CLSM, confocal laser scanning microscope; RWM, round window membrane; DAPI, 4′,6-diamidino-2-phenylindole; PLGA NPs, poly (lactic-co-glycolic acid) nanoparticles.

pathway and caveolae-mediated endocytosis pathway, as shown in Figure 8A. The endocytosis of NPs was barely effected by the presence of chlorpromazine; so the clathrin-dependent endocytosis pathway was not responsible for the NP endocytosis (Figure 8A).

Golgi apparatus-mediated exocytosis of NPs

In general, lysosomes are not the only destination of nanocarriers.[8] Besides the digestive endolysosomal pathway, nanomaterials exit from cells through exocytosis-related organelles, that is, Golgi apparatus and ER.[10] Compared to the control group, both BFA and MON inhibited the transport amount of NPs in the perilymph, as shown in Figure 8B.

Thus, the Golgi apparatus may be involved in the exocytosis of NPs.

Intracellular trafficking of NPs in RWM

After the entry of NPs into cells, various organelles, such as lysosomes, ER and Golgi apparatus, fused with the internalized vesicles. To analyze the intracellular location of NPs, LysoTracker Red was used to detect the entrapment of NPs in lysosomes by ZEN colocalization software (Carl Zeiss Meditech AG, Jena, Germany). NPs were colocalized with lysosomes, with the merged image appearing as an orange signal, as shown in Figure 9A. The colocalization scatterplots (Figure 9B), colocalization mask images showing only overlapping pixels (Figure 9C), and the quantitative
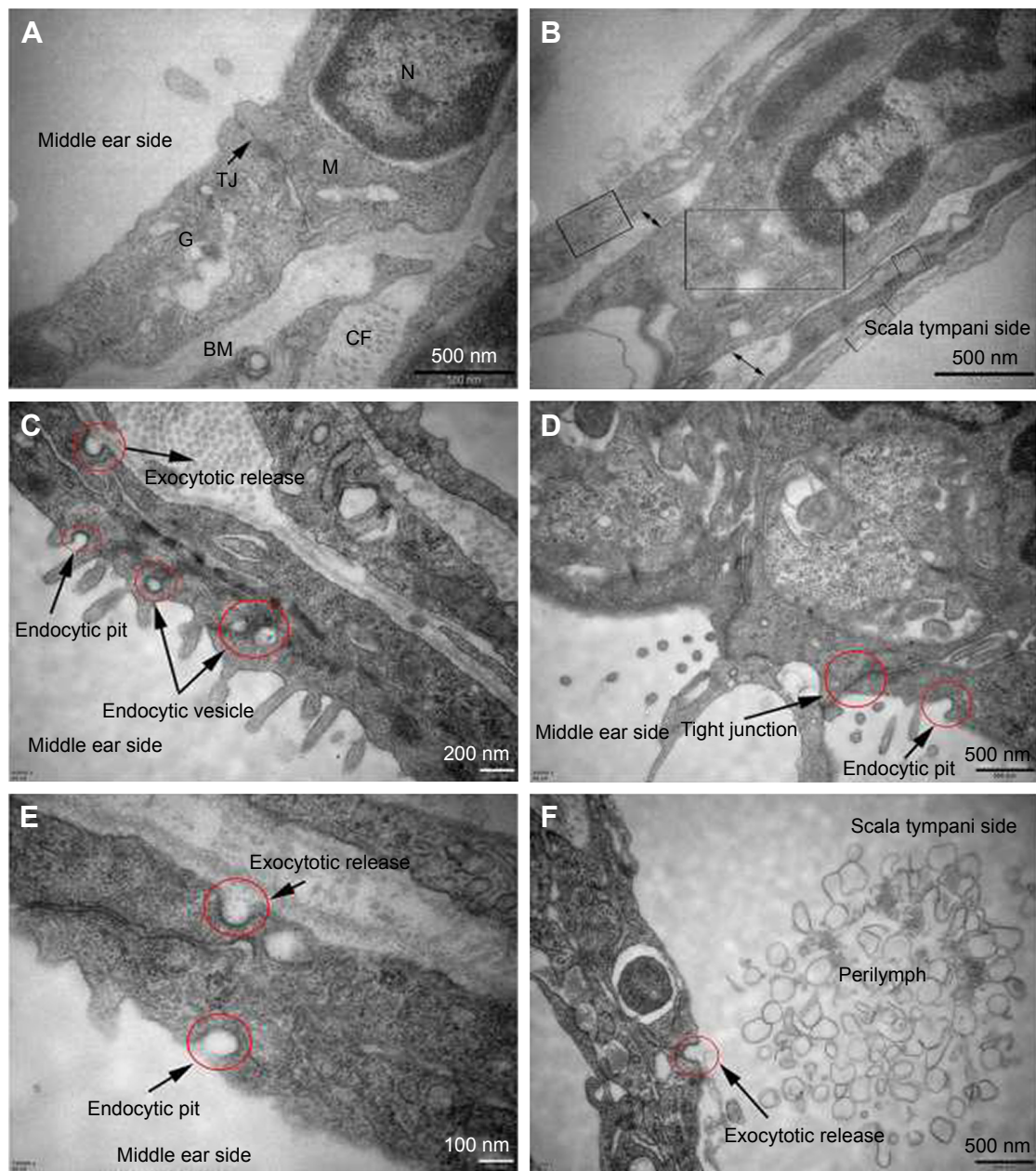
Figure 6 TEM images of RWM in the control group and intratympanic injection of PLGA NPs group. Subcellular characteristics of RWM in the control group (**A**, **B**) and intratympanic injection of PLGA NPs for 30-minute group (**C**–**F**). (**A**) Tight junctions which sealed the paracellular space between adjacent cells and a variety of organelles were found in the RWM outer epithelium layer. (**B**) There were four layers in the RWM inner epithelium layer, and each layer was marked by a rectangular frame; the large extracellular spaces were marked by double arrows. (**C**) Successive transport behavior, including endocytic pit, intracellular vesicles, and exocytic pit, was captured. Extensive endocytic and exocytic behaviors (**D**–**F**) and closed tight junction (**D**) in the RWM outer epithelium layer. Exocytotic release behavior was also observed in the RWM inner epithelium layer (**F**).

Abbreviations: TEM, transmission electron microscope; RWM, round window membrane; PLGA NPs, poly (lactic-co-glycolic acid) nanoparticles; M, mitochondria; N, nucleus; TJ, tight junction; G, Golgi apparatus; BM, basement membrane; CF, collagenous fiber.

colocalization parameters (Figure 9D) illustrated the actual transport of PLGA NPs to lysosomes.

Discussion

RWM surface preparation has been used to test the permeability of inner ear drug delivery systems through the membrane.

El Kechai et al[19] employed this method to evaluate the permeability of hyaluronic acid liposomal gel, but a small number of RWM samples was obtained due to immature sampling technology, despite having many involved animals. Actually, the integrity of RWM would not collapse during the extraction of the surrounding bone, which increases the success
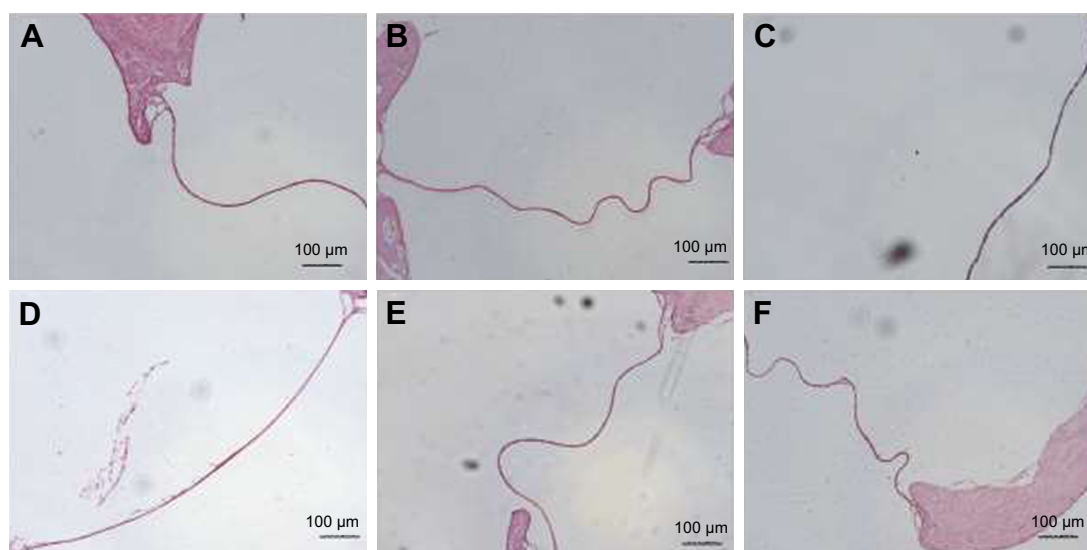
Figure 7 Safety evaluation of various inhibitors using paraffin sections of RWM. Control group (**A**), colchicine (**B**), MβCD (**C**), chlorpromazine hydrochloride (**D**), MON (**E**), and BFA (**F**).
Abbreviations: RWM, round window membrane; MβCD, methyl-β-cyclodextrin; MON, monensin sodium salt; BFA, brefeldin A.

rate of the experimental operation. Shih et al also utilized this method to assess whether microbubble ultrasound facilitated drug delivery to the inner ear, which failed to detailedly distinguish the outer epithelium layer, connective tissue, and inner epithelium layer of RWM using CLSM z-stack images.[20] These problems were circumvented in our study. As a useful technique, this strategy can evaluate the efficiency of inner ear topical drug delivery system.

As indicated by a small loss of coumarin-6 fluorescence under acidic and neutral conditions in 4 hours, coumarin-6 was an effective probe in intracellular milieus with various pH values. PLGA NPs have been postulated to enter the inner

ear mainly through RWM based on indirect evidences such as perilymph pharmacokinetics studies and distribution of NPs in the inner ear tissue.[21,22] In contrast, by observing RWM samples by CLSM in the z-stack scanning model, we can directly visualize the entry of PLGA NPs across RWM.

PLGA NPs penetrated across RWM via the transcellular pathway, not the paracellular pathways. Probably, the overall surface area defined by the transcellular route accounts for most of the surface area of the middle ear side of RWM.[23] Correspondingly, endocytosis is a general route of NP internalization.[24] When NPs approach the epithelium barrier, they try optionally to seek a suitable interaction
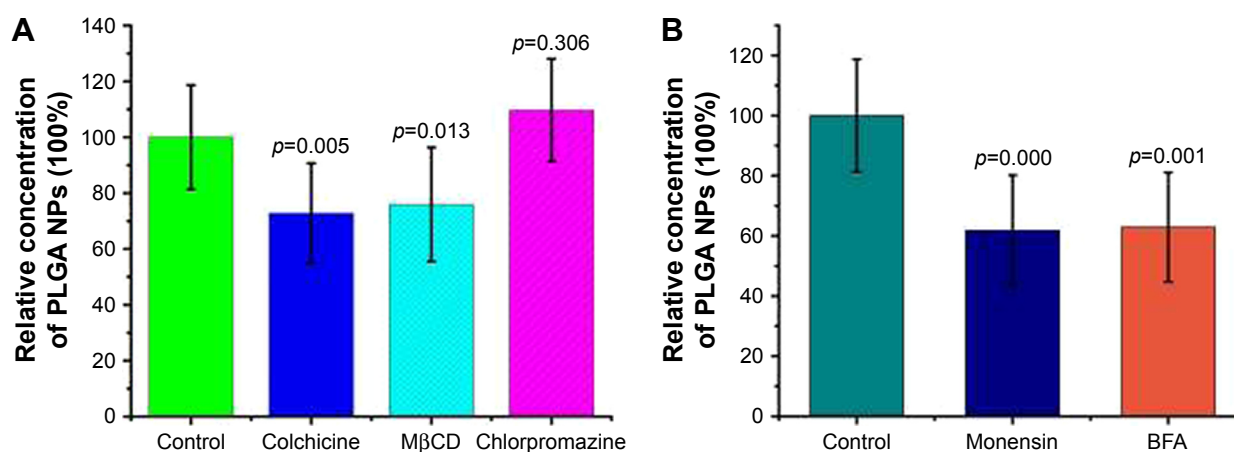

Figure 8 Endocytosis and exocytosis mechanisms of PLGA NPs across RWM. The effects of different endocytosis inhibitors (**A**) and exocytosis inhibitors (**B**) on the transport of PLGA NPs were monitored by HPLC. Incubation with only PBS represented the control and the related data were set as 100%. All data were compared to the control using ANOVA.
Abbreviations: PLGA NPs, poly (lactic-co-glycolic acid) nanoparticles; RWM, round window membrane; HPLC, high-performance liquid chromatography; PBS, phosphate-buffered saline; ANOVA, analysis of variance; MβCD, methyl-β-cyclodextrin; BFA, brefeldin A.
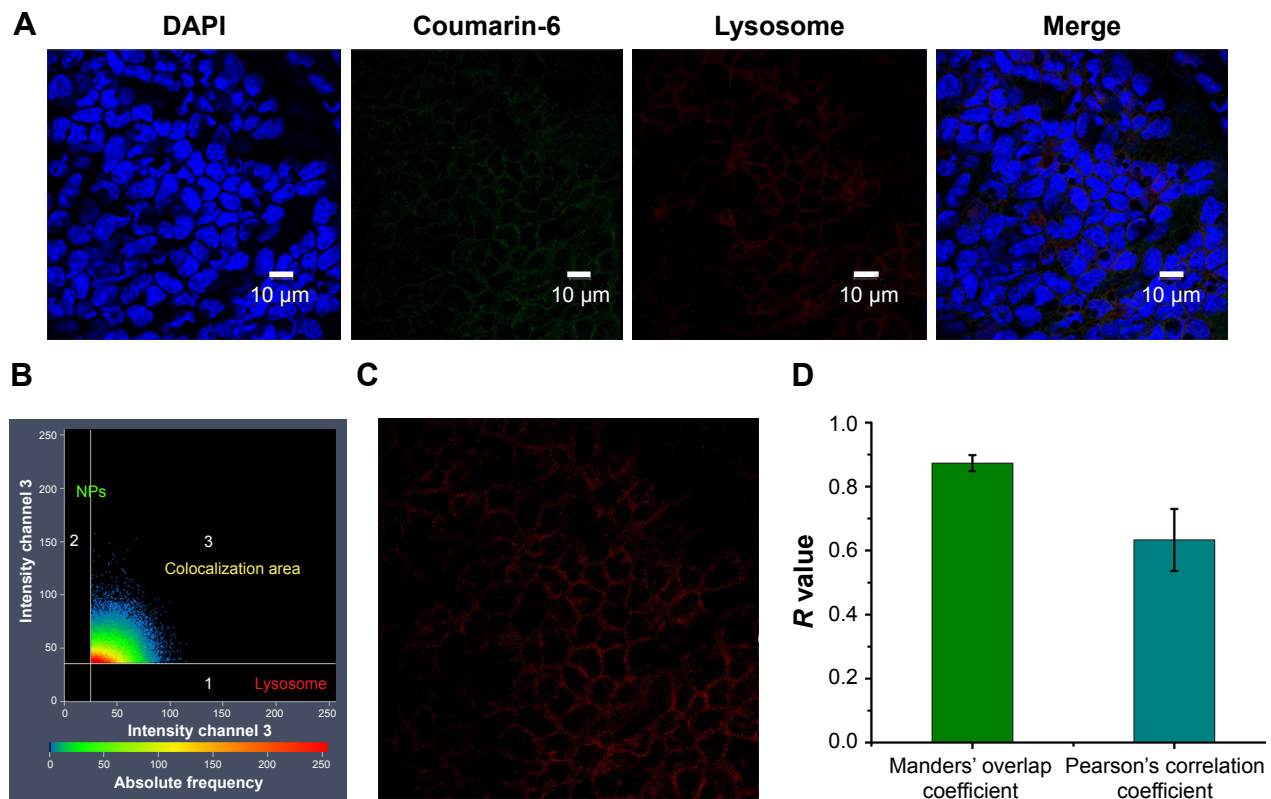
Figure 9 Colocalization analysis of PLGA NPs with lysosomes. CLSM micrographs of outer epithelium cells of RWM after intratympanic injection of PLGA NPs for 30 minutes (**A**). Colocalization scatterplots of PLGA NPs with lysosomes (**B**). Colocalization mask images showing only overlapping pixels **(C)**. Quantitative colocalization parameters of PLGA NPs with lysosomes by measuring Manders' overlap coefficient and Pearson's correlation coefficient **(D)**.
Abbreviations: PLGA NPs, poly (lactic-co-glycolic acid) nanoparticles; CLSM, confocal laser scanning microscope; RWM, round window membrane; DAPI, 4′,6-diamidino-2-phenylindole.

site. We herein verified that macropinocytosis was the main internalization pathway for PLGA NPs. NPs with sizes in the range of 200 nm were internalized through ruffling of the plasma membrane to form macropinosomes of around 0.5–10 μm via the macropinocytosis pathway.[8] Caveolae-associated endocytosis was also involved in the PLGA NP transport. After separating from the cell membrane, the endocytosed vesicle formed a special structure with diameter of about 50–80 nm, referred to as caveosome. Clathrin-mediated endocytosis is a classical endocytosis pathway. Extracellular substances are packed by the cell membrane, forming clathrin-coated pits that then interact with the vesicle system to move around in cells.[25] Our study suggested that clathrin-mediated endocytosis was not responsible for the NP entry into RWM.

After entering cells, NPs are transported among multiple organelles through vesicles system, of which endosomes are the primary intracellular organelles encountered.[26] In general, NPs merge with early endosomes firstly, mature into late endosomes, and fuse with lysosomes ultimately, a limiting step for NPs to exert pharmacological actions.[27] Since NPs

are prone to be degraded in lysosomes due to abundant hydrolytic enzymes, lysosome becomes the endpoint for most nanocarriers which cannot be transported further.[28] In this study, the colocalization of PLGA NPs with lysosomes made us envision that endocytosed NPs could be transported from early endosomes to lysosomes via the early endosome/late endosome/lysosome pathway. Most NPs, such as PLGA NPs, micelles, chitosan NPs, and microgels, can be entrapped by this classical degradation system.[29] Nevertheless, the cytoplasm of RWM is not the destination of NPs. NPs should escape from lysosomes, and as many NPs as possible should move across the RWM into the perilymph. Consequently, it is of great significance to engineer effective inner ear nano-drug delivery systems capable of endosomal escape.

With prolonged time, RWM not only internalized PLGA NPs, but also continuously discharged them out of cells to the perilymph. Besides the degradative early endosome/late endosome/lysosome pathway, vesicles were also transferred to the Golgi apparatus and ER, also known as the retrograde trafficking pathway avoiding the lysosomal environment and then mediating NPs out of the cell membrane. BFA,
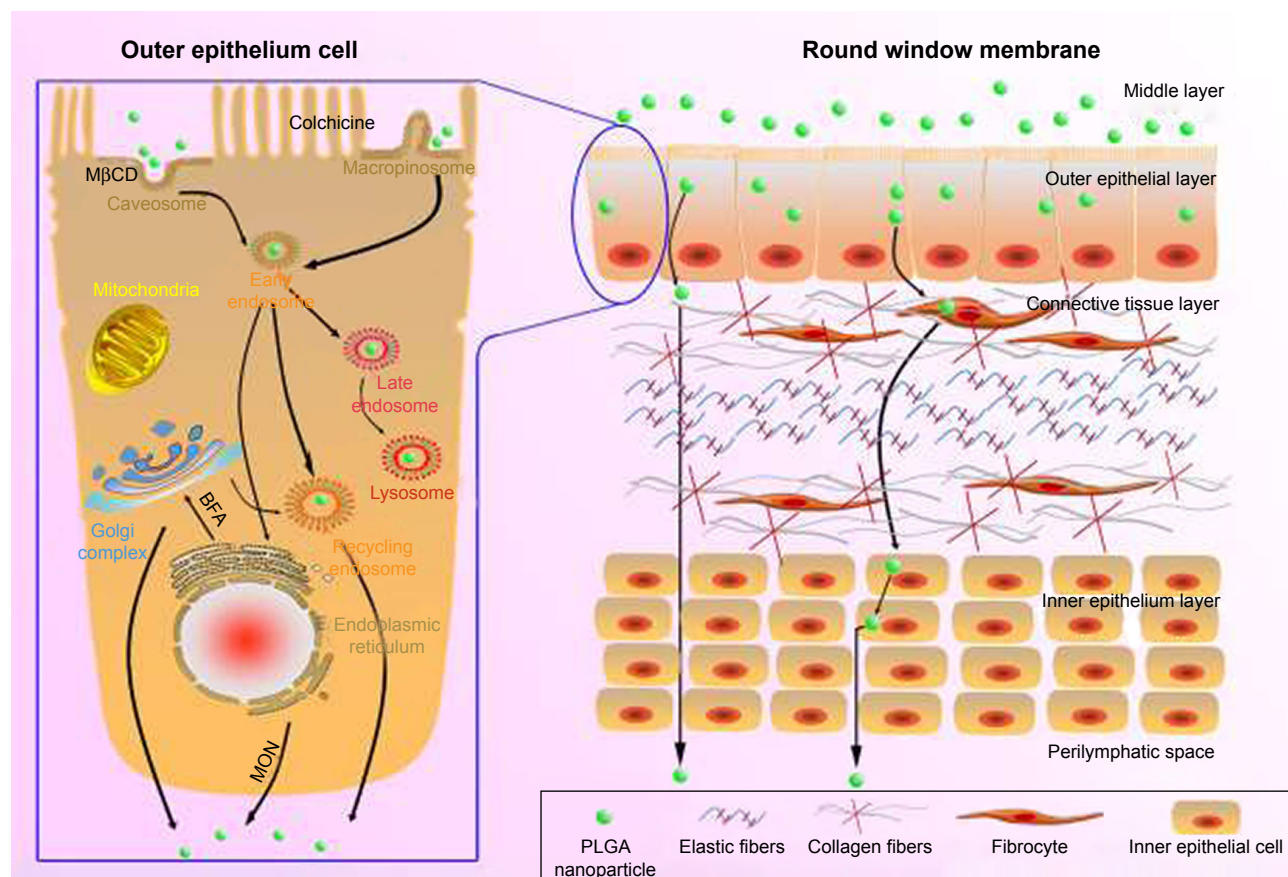
Figure 10 Schematic diagram of the transport pathways of NPs in the outer epithelium of the RWM (left) and the passage loci of PLGA NPs in the RWM (right). Black solid arrows indicate the pathways that were directly or indirectly proven in this study.
Abbreviations: PLGA NPs, poly (lactic-co-glycolic acid) nanoparticles; RWM, round window membrane; MβCD, methyl-β-cyclodextrin; MON, monensin sodium salt; BFA, brefeldin A.

an antibiotic, inhibits the transport of vesicles from ER to the Golgi apparatus. MON can disrupt the Golgi apparatus, thereby efficiently blocking the transfer of vesicles to the cell membrane. In this study, ER/Golgi apparatus and Golgi apparatus/cell membrane pathways were both blocked when RWM samples were treated with BFA and MON. Hence, in-depth studies are needed to markedly promote NP entry into the perilymph relying on the retrograde trafficking pathway.

Until now, we have depicted the transport routes of PLGA NPs in RWM (Figure 10). NPs traversed multiple pathways including caveolae-mediated endocytosis and macropinocytosis in the outer epithelium layer of the membrane barrier, indicating that the endocytosis routes were nonspecific. Then, NPs-loaded vesicles were involved in the early endosome/late endosome/lysosome pathway. Additionally, the exocytosis of NPs was regulated by the Golgi apparatus and ER via the ER/Golgi apparatus/cell membrane exocytic pathway. In fact, the entire RWM crossing process of PLGA NPs included entry into the outer epithelium cells through endocytosis,

intracellular trafficking, exit from the basolateral membrane of outer epithelium cells through exocytosis, and final transport to the connective tissue layer and inner epithelium layer. Unlike the outer epithelium layer of RWM, once a substance arrived at the connective tissue layer, it moved directly through "gaps" among inner epithelial cells toward the scala tympani.[1] Collectively, the whole transport trajectory of NPs in RWM has been clarified herein to provide avenues for the optimization of inner ear nano-drug delivery system.

In the past years, various functional moieties have been incorporated into NP design to overcome biological barriers. Based on the findings in this study, we recommended to 1) open tight junctions, 2) enhance endocytosis, and 3) facilitate endosomal escape. The tight junctions of the epithelium barrier have been targeted in previous literatures. González-Mariscal et al reviewed the strategies employed to disrupt tight junctions, including antibodies, peptides, miRNAs, melittin, and chemicals that enhance drug delivery via the paracellular pathway.[30] NPs based on chitosan or its derivatives can open tight junctions transiently and reversibly.[31]

Liu et al employed a trimethyl chitosan-based core which opened tight junctions to overcome the epithelium barrier.[32] Enslin et al utilized the synergistic effect of melittin and trimethyl chitosan, which reduced their doses and related toxic effects.[33] Beyond that, several strategies, including cell penetrating peptides (CPPs), positive surface charge, and ligands, have been adopted to trigger the endocytosis of NPs. Particularly, modifying the drug carriers with CPPs has been successfully applied to various drug delivery systems. Steinbach et al found that decorating PLGA NPs with CPPs strikingly enhanced the cell binding and internalization of NPs.[34] Sánchez-Navarro et al reviewed various CPPs that facilitated biotherapeutics to transport across the intestinal barrier.[35] Last but not least, endosomal escape can also improve the effectiveness of drug delivery systems by protecting drug carriers from the acidified and degradative lysosome system. Biological toxins, such as Shiga toxin, ricin, and cholera, have been exploited to escape endolysosomal compartments.[36] Deng et al developed pH-reactive charge reversal NPs that allowed endosomal escape.[37] Paka and Ramassamy found that NPs anchored with glutathione escaped the endocytosis pathway of macropinocytosis, without being entrapped into lysosomes.[38] Besides the methods described here, NP transport can also be promoted by altering particle sizes and shapes as well as by surface modification with targeting ligands. Inner ear drug delivery can be optimized based on achievements in the design of nano-drug delivery systems.

Conclusion

This study analyzed the first-generation nanomaterials derived from an urgent requirement to push through the limitations of low-permeability drugs across the biological barrier. With simplified design, these NPs were evaluated as carriers for drug solubilization with the potential to improve the bioavailability of free drugs, providing an effective means for optimizing drug delivery. Currently, it is evident that this field is transitioning toward more rational approaches that take into consideration the transport mechanism of NPs in the epithelium barrier. Overall, enhanced understanding of RWM crossing processes of PLGA NPs may offer avenues for next-generation intelligentialized and functionalized NPs. Notably, NPs-based drug delivery systems should be considered a viable and commonplace strategy, as opposed to a promising option, for the treatment of inner ear diseases.

Acknowledgments

Disclosure

The authors report no conflicts of interest in this work.

References

1. Zou J, Sood R, Zhang Y, Kinnunen PK, Pyykkö I. Pathway and morphological transformation of liposome nanocarriers after release from a novel sustained inner-ear delivery system. *Nanomedicine*. 2014;9(14):2143–2155.
2. Goycoolea MV. Clinical aspects of round window membrane permeability under normal and pathological conditions. *Acta Otolaryngol*. 2001;121(4):437–447.
3. Goycoolea MV, Lundman L. Round window membrane. Structure function and permeability: a review. *Microsc Res Tech*. 1997;36(3):201–211.
4. Zhang Y, Su H, Wen L, Yang F, Chen G. Mathematical modeling for local trans-round window membrane drug transport in the inner ear. *Drug Deliv*. 2016;23(8):3082–3087.
5. Alonso MJ. Nanomedicines for overcoming biological barriers. *Biomed Pharmacother*. 2004;58(3):168–172.
6. Cai H, Wen X, Wen L, et al. Enhanced local bioavailability of single or compound drugs delivery to the inner ear through application of PLGA nanoparticles via round window administration. *Int J Nanomedicine*. 2014;9:5591–5601.
7. Chen G, Zhang X, Yang F, Mu L. Disposition of nanoparticle-based delivery system via inner ear administration. *Curr Drug Metab*. 2010;11(10):886–897.
8. Ge X, Jackson RL, Liu J, et al. Distribution of PLGA nanoparticles in chinchilla cochleae. *Otolaryngol Head Neck Surg*. 2007;137(4):619–623.
9. Wen X, Ding S, Cai H, et al. Nanomedicine strategy for optimizing delivery to outer hair cells by surface-modified poly (lactic/glycolic acid) nanoparticles with hydrophilic molecules. *Int J Nanomedicine*. 2016;11:5959–5969.
10. He B, Lin P, Jia Z, et al. The transport mechanisms of polymer NPs in Caco-2 epithelial cells. *Biomaterials*. 2013;34(25):6082–6098.
11. He B, Jia Z, Du W, et al. The transport pathways of polymer NPs in MDCK epithelial cells. *Biomaterials*. 2013;34(17):4309–4326.
12. Pinto-Alphandary H, Aboubakar M, Jaillard D, Couvreur P, Vauthier C. Visualization of insulin-loaded nanocapsules: in vitro and in vivo studies after oral administration to rats. *Pharm Res*. 2003;20(7):1071–1084.
13. Cartiera MS, Johnson KM, Rajendran V, Caplan MJ, Saltzman WM. The uptake and intracellular fate of PLGA nanoparticles in epithelial cells. *Biomaterials*. 2009;30(14):2790–2798.
14. Qaddoumi MG, Ueda H, Yang J, Davda J, Labhasetwar V, Lee VH. The characteristics and mechanisms of uptake of PLGA nanoparticles in rabbit conjunctival epithelial cell layers. *Pharm Res*. 2004;21(4):641–648.
15. Pelkonen O, Boobis AR, Gundert-Remy U. In vitro prediction of gastrointestinal absorption and bioavailability: an experts' meeting report. *Eur J Clin Pharmacol*. 2001;57(9):621–629.
16. Conner SD, Schmid SL. Regulated portals of entry into the cell. *Nature*. 2003;422(6927):37–44.
17. Pratten MK, Lloyd JB. Effects of temperature, metabolic inhibitors and some other factors on fluid-phase and adsorptive pinocytosis by rat peritoneal macrophages. *Biochem J*. 1979;180(3):567–571.
18. Sun X, Yau VK, Briggs BJ, Whittaker GR. Role of clathrin-mediated endocytosis during vesicular stomatitis virus entry into host cells. *Virology*. 2005;338(1):53–60.
19. El Kechai N, Mamelle E, Nguyen Y, et al. Hyaluronic acid liposomal gel sustains delivery of a corticoid to the inner ear. *J Control Release*. 2016;226:248–257.
20. Shih CP, Chen HC, Chen HK, et al. Ultrasound-aided microbubbles facilitate the delivery of drugs to the inner ear via the round window membrane. *J Control Release*. 2013;167(2):167–174.

21. Long W, Zhang S, Wen L, Mu L, Yang F, Chen G. In vivo distribution and pharmacokinetics of multiple active components from Danshen and Sanqi and their combination via inner ear administration. *J Ethnopharmacol*. 2014;156:199–208.

22. Zou J, Hannula M, Misra S, et al. Micro CT visualization of silver nanoparticles in the middle and inner ear of rat and transportation pathway after transtympanic injection. *J Nanobiotechnology*. 2015;13:5.

23. Pade V, Stavchansky S. Estimation of the relative contribution of the transcellular and paracellular pathway to the transport of passively absorbed drugs in the Caco-2 cell culture model. *Pharm Res*. 1997;14(9):1210–1215.

24. Mrsny RJ. Lessons from nature: "pathogen-mimetic" systems for mucosal nano-medicines. *Adv Drug Deliv Rev*. 2009;61(2):172–192.

25. Pucadyil TJ, Schmid SL. Conserved functions of membrane active GTPases in coated vesicle formation. *Science*. 2009;325(5945):1217–1220.

26. Wang C, Wang Y, Li Y, et al. A nanobuffer reporter library for fine-scale imaging and perturbation of endocytic organelles. *Nat Commun*. 2015;6:8524.

27. Fan W, Xia D, Zhu Q, Hu L, Gan Y. Intracellular transport of nanocarriers across the intestinal epithelium. *Drug Discov Today*. 2016;21(5):856–863.

28. Raj DBTG, Khan NA. Designer nanoparticle: nanobiotechnology tool for cell biology. *Nano Converg*. 2016;3(1):22.

29. Zhang J, Zhang X, Liu G, et al. Intracellular trafficking network of protein nanocapsules: endocytosis, exocytosis and autophagy. *Theranostics*. 2016;6(12):2099–2113.

30. González-Mariscal L, Posadas Y, Miranda J, et al. Strategies that target tight junctions for enhanced drug delivery. *Curr Pharm Des*. 2016;22(35):5313–5346.

31. Mukhopadhyay P, Mishra R, Rana D, Kundu PP. Strategies for effective oral insulin delivery with modified chitosan nanoparticles: a review. *Prog Polym Sci*. 2012;37(11):1457–1475.

32. Liu M, Zhang J, Zhu X, et al. Efficient mucus permeation and tight junction opening by dissociable "mucus-inert" agent coated trimethyl chitosan nanoparticles for oral insulin delivery. *J Control Release*. 2016;222:67–77.

33. Enslin GM, Hamman JH, Kotzé AF. Intestinal drug absorption enhancers: synergistic effects of combinations. *Drug Dev Ind Pharm*. 2008;34(12):1343–1349.

34. Steinbach JM, Seo YE, Saltzman WM. Cell penetrating peptide-modified poly (lactic-co-glycolic acid) nanoparticles with enhanced cell internalization. *Acta Biomater*. 2016;30:49–61.

35. Sánchez-Navarro M, Garcia J, Giralt E, Teixidó M. Using peptides to increase transport across the intestinal barrier. *Adv Drug Deliv Rev*. 2016;106(Pt B):355–366.

36. Walker WA, Tarannum M, Vivero-Escoto JL. Cellular endocytosis and trafficking of cholera toxin B-modified mesoporous silica nanoparticles. *J Mater Chem B Mater Biol Med*. 2016;4(7):1254–1262.

37. Deng X, Wang Y, Zhang F, et al. Acidic pH-induced charge-reversal nanoparticles for accelerated endosomal escape and enhanced microRNA modulation in cancer cells. *Chem Commun (Camb)*. 2016;52(15):3243–3246.

38. Paka GD, Ramassamy C. Optimization of curcumin-loaded PEG-PLGA nanoparticles by GSH functionalization: investigation of the internalization pathway in neuronal cells. *Mol Pharm*. 2016;14(1):93–106.